Versatile three-dimensional cryogenic micropositioning device

J. Heil, A. Böhm, M. Primke, and P. Wyder
Hochfeld-Magnetlabor, Max-Planck-Institut für Festkörperforschung and Centre National de la Recherche Scientifique, B. P. 166, 25 Avenue des Martyrs, F-38042 Grenoble Cedex 9, France

(Received 15 August 1995; accepted for publication 15 October 1995)

A simple design for a mechanically driven three-dimensional cryogenic micropositioner is presented. The design is based on a parallelogram structure constructed from leaf springs and wires. Actuation is achieved by the elastic deformation of the parallelogram by screws. Positions within a volume of roughly $(2\ \mathrm{mm})^3$ are attainable. The precision and reproducibility of positioning are in the μm-range. The deviations from linearity are smaller than 10% for the whole working range and the deviation from orthogonality is smaller than 3°. Calibration measurements performed on a Cu-mesh with a lattice constant of 60 μm are presented. In an experiment investigating the ballistic transport of carriers in the semimetal Bi, two such devices are used. The first one is used as a scanning unit for an optical fiber and the second one is used as micropositioner for a Cu point contact. © *1996 American Institute of Physics.* [S0034-6748(96)05301-1]

I. INTRODUCTION

In the last decade a considerable number of scanning probe techniques (SPM) have been developed.[1,2] Common to all is the need for a positioning or a scanning movement of the probing tool with respect to the investigated system, the range and the resolution depending on the method applied. For high resolution techniques like scanning tunneling microscopy and its spin-offs[3–6] mechanical scanners incorporating piezoelectric actuators are the appropriate choice, although a coarse positioning unit is needed to bring the probe and the investigated system within working distance. This coarse approach is usually a purely mechanical, electromechanical or a stepped piezoelectric system.

For SPM techniques applied to the mm range, piezoelectric actuators are not favorable.[7–12] To access mm ranges, either their dimensions are inconveniently large, their deformation has to be amplified by lever systems or they have to be combined with multimorph elements.[13] In addition problems inherent to piezoelectric ceramics like creep, hysteresis and nonlinearity become more and more important, the larger the excursion of the actuators and the lower the scan rates are. Therefore, feedback techniques have to be used in order to enable such a system to position the probe to a specified location.

In order to avoid these problems mechanically driven scanners can be employed.[14–17] They offer easy construction, ease of operation (they can even be operated manually) and stable positioning while inactive. Among the disadvantages are of course vibrations during scanning operation and the necessity of a mechanical access to the experimental region.

We have constructed a mechanical micropositioning unit, which is able to position a probe in three dimensions over a full range of approximately 2 mm with a resolution and reproducibility in the μm range. Its design and features, calibration measurements and applications are presented here.

II. DESIGN OF THE MICROPOSITIONER

Figure 1 shows a schematic representation of the mechanical scanner. The key element of this construction is a three-dimensional parallelogram composed of 5 leaf springs and a wire cross. To actuate the probe support to a desired position, three brass screws are used, each associated to the motion in the x-,y- and z-directions, respectively. A conical hole is drilled into the lower end of each screw. A bronze wire of 0.6 mm diameter with its upper end ground to a tiny hemisphere can rotate freely in this hole, forming a needle joint. In the case of motion in the x- and y-directions this wire transmits the longitudinal motion of the screw to a lever, to which it is fixed by soft soldering. The lever then transforms the screw motion into a bending of the leaf spring in the x- or y-direction. For movement in z-direction the wire is directly soldered to the corresponding leaf spring. The screws work against a restoring force. For x- and y-motion this force is supplied by a similar lever mechanism situated on the complementary leaf spring of the parallelogram. It is generated by helical springs wound from a bronze wire of 0.6 mm diameter and is transmitted to the lever via a string from artificial silk. For z-motion, the restoring force is directly applied to the leaf spring, to which the actuating force is applied. We would have preferred to apply the actuating and restoring forces to approximately the same working point for all axes in order to have the forces canceled within a single mechanical element and to avoid the whole parallelogram structure being set under permanent considerable mechanical tension. However up to now only the solution presented here has been realized because of the small space available (cylindrical tube with 42 mm inner diameter).

The probe is attached to a support which is suspended within the leaf spring parallelogram by bronze wires of 0.4 mm diameter. Movements of the leaf spring structure are transmitted via these wires to the support. Since the whole structure is under tension, this wire cross is quite rigid, contrary to its appearance. Due to the symmetry of the design (apart from the z-motion) the movements of the support in the x- and y-directions are orthogonal and decoupled from each other for small displacements. The continuous tension in the springs takes virtually all mechanical play out of the system.

In an earlier version of the scanner the screws had hemi-

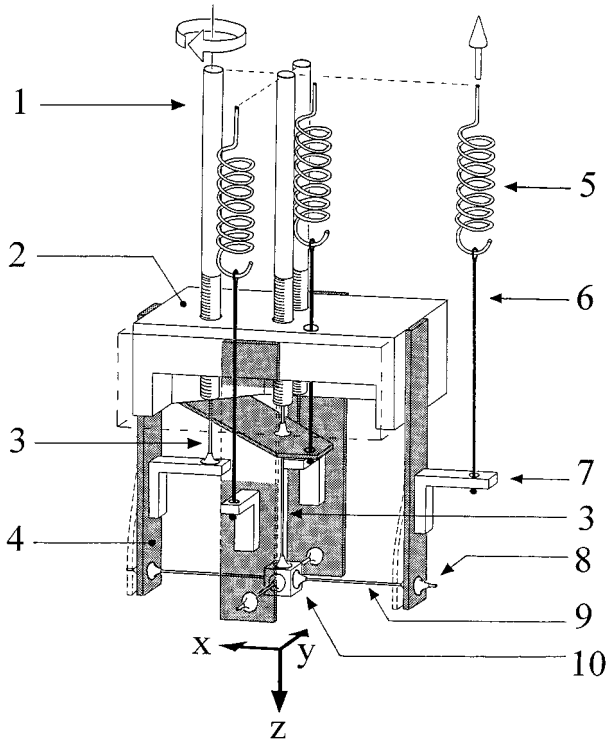

FIG. 1. Schematic representation of the scanner mechanics: (1) brass screw (M3 × 350 μm), (2) base structure made from brass (partly cut away), (3) bronze wire (0.6 mm diameter), (4) bronze leaf spring (0.3 mm thickness, shown partly transparent), (5) helical spring made from bronze wire (0.6 mm diameter), (6) string from artificial silk, (7) brass lever, (8) soft soldering, (9) bronze wire (0.4 mm diameter), (10) probe support. Turning the x screw results in a deformation of the structure indicated by the dashed lines. See the text for explanation.

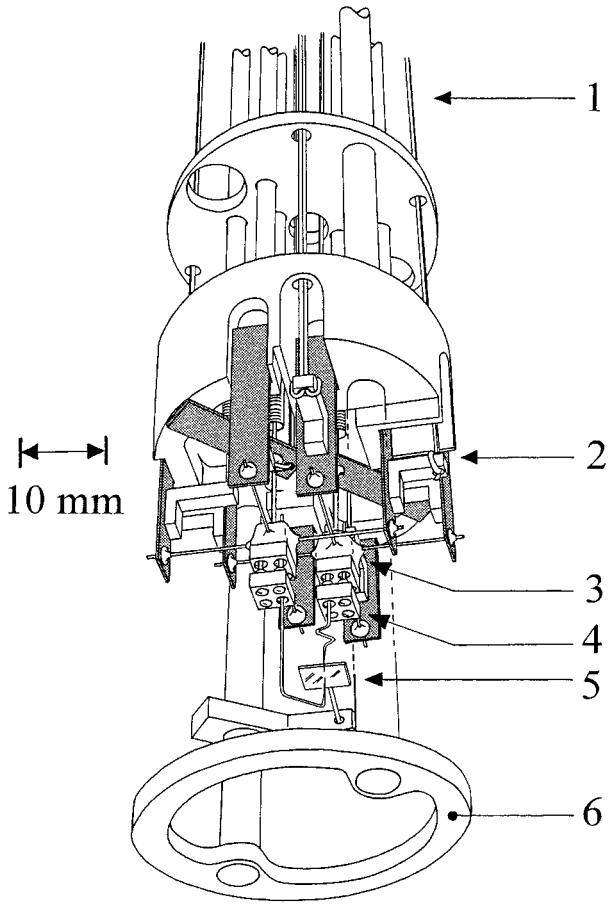

FIG. 2. Setup used for the experiments presented here. Two scanners of the kind shown in Fig. 1 are mounted together on one base structure to allow two-probe measurements on one sample: (1) control tubes and strings to the springs (springs not shown), (2) scanner, (3) probe supports produced from IC-pins cast with low temperature epoxy, (4) IC-pin connectors with mounted point contacts plugged into the supports, (5) sample mounted on a 1 mm diameter wire, can be pivoted out of the working region, (6) ring for mechanical protection.

spheric lower ends pushing the levers directly. This solution was abandoned because of the sensitivity of the system to lateral motions of the screw head due to play in the threads. The present construction avoids this problem because a lateral movement of the screw leads in first order only to a bending of the wire, but not to an unwanted longitudinal displacement of the wire. In this first scanner version, the restoring force was supplied by the deformation of the leaf springs themselves. The disadvantage is that the restoring force depends strongly on the position. The advantage of this approach is the smaller number of parts involved and the greater compactness and rigidity of the construction. In fact, the present design suffers from sensitivity to vibrations, since the string-spring combination represents a mechanical oscillator with a high quality and a low resonance frequency susceptible to mechanical pick up.

Figure 2 shows our setup composed of two scanners like those presented in Fig. 1 fitted into one another and displaced 7 mm, 7 mm and 3 mm from each other in the x-,y- and z-directions, respectively. The two probe supports are glued together from four IC-socket contacts. One of the pins of the socket is soldered to the wire cross of the scanner while the others are left as probe contacts. To stabilize the probe support on the cross the empty spaces are cast with a low temperature epoxy.[18] The probes used during the experiments, usually an optical fiber and point contacts, are attached to similar four pin connectors and can easily be employed or exchanged by plugging them into the supports.

The construction presented here fits into the tail of a glass cryostat with an internal diameter of 42 mm. It is operated in immersion in liquid ^{4}He down to temperatures of $T=1.5$ K. Adjustment of the probes with respect to the sample is performed under operating conditions under optical control by a video microscope from outside the Dewar. The resolution of the optics is limited to about 20 μm by the quality of the glass tubes of the cryostat allowing only small apertures of roughly 1.5 mm at working distances in the range of 50 mm. Less than 50 μm overall distortion is observed during (slow) cool down if a more or less homogeneous temperature distribution is established. The screws are connected to stainless steel tubes of 3 mm outer diameter used as flexible shafts. They are fed through squeezable O-ring seals at the top flange of the Dewar. They can be controlled manually or be coupled to stepper motors; in the first case ten-turn helipots attached to the tubes can be used as position encoders.

III. TEST AND CALIBRATION

Calibration measurements were performed in order to check the performance of the scanner. The beam of an Ar-ion

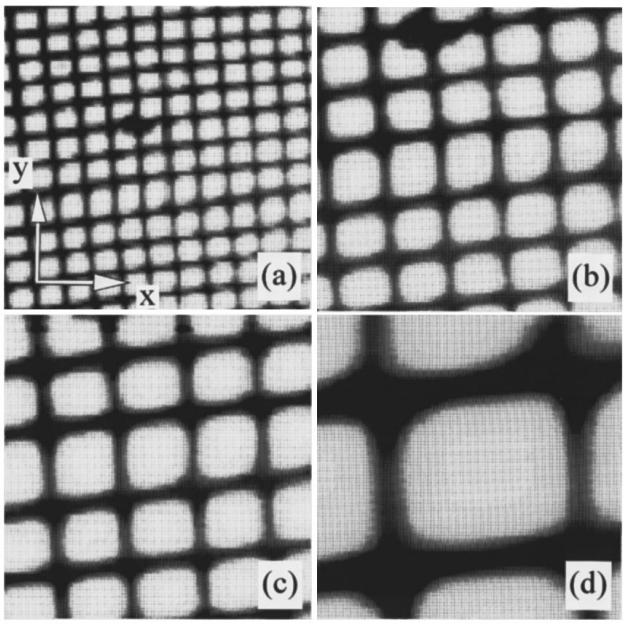

FIG. 3. The voltage generated by a photodiode illuminated through a Cu mesh with a lattice constant of $g=60$ μm is represented in grey scale as a function of the position of the illuminating fiber: (a) frame (1000×800) steps corresponding to (660 μm)^2, 10 steps between data points, (b) frame (500×400) steps corresponding to (330 μm)^2, 5 steps between data points, (c) frame (400×320) steps corresponding to (265 μm)^2, 5 steps between data points, (d) frame (160×128) steps corresponding to (110 μm)^2, 2 steps between data points.

laser was fed into an optical fiber with a core diameter of 15 μm. The fiber end was used to illuminate a photodiode through a Cu-mesh with a lattice constant of $g=60$ μm. The fiber end was brought as close as possible ($\approx$20 μm) to the mesh, the diameter of the illuminated area (full-width at half-maximum) is estimated to be 15 μm to 20 μm. To avoid thermal drift effects which disturb the measurements considerably when done in air at ambient conditions, the calibrations were performed in the cryostat in immersion in liquid N_2 at $T=77$ K. The acquisition time for a data set composed from (100×100) data points is typically 1 hour. The screws were driven by stepping motors with 1000 steps per revolution. The voltage V_{ph} generated by the photodiode was then recorded as a function of the position (x,y) of the optical fiber. The result is shown in Fig. 3, $V_{ph}(x,y)$ is presented in grey scale, the brightness being a linear function of the signal. Apart from a slight ''barrel''-shaped distortion visible in the largest frame, the appearance of the images is quite regular. The following characteristics for the scanner are derived from these measurements: sensitivity: 0.66 μm/step (1 step corresponds to 0.36°), in the x-direction and 0.82 μm/step in the y-direction. This (relatively large) asymmetry probably results from the soft solderings and the castings which cannot be made completely identical: Resolution$\approx$10 μm (in our case limited by the extension of the illuminated area); deviation from linearity $<$10% per full range, deviation from orthogonality $<3°$ in the full range; reproducibility of positioning <2 μm [estimated from Fig. 3(d), possibly even better].

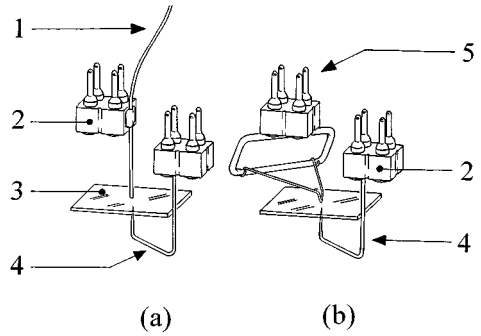

FIG. 4. Probe and sample configuration for (a) thermal excitation of carriers by illumination and (b) injection of carriers through a point contact: (1) optical fiber (scanned), (2) 4-pin IC-connector, (3) sample, (4) collector point contact etched from 100 μm diameter Cu-wire (fixed), (5) emitter point contact assembly bent from 100μm diameter Cu-wire mounted on IC-connector (scanned).

IV. APPLICATIONS

The setup was used to investigate the ballistic transport of carriers in a Bi single crystal.[19]

If pure metal crystals are cooled down to very low temperatures T, the electronic mean free path l^* can be in the mm range, so ballistic transport through macroscopic samples is possible. Nonequilibrium carriers are generated by the illumination of a small surface area (hot spot) or by injection through a point contact (PC), the emitter (E) spot is welded to one of the sample surfaces. The carriers spread out through the crystal, hit the opposite sample surface and are detected by a (second) PC, the so-called collector (C).

Figure 4 shows the probe and sample configuration used for this experiment. The hot spot can simply be scanned across the c-surface of the sample. The laser beam is chopped with a frequency of roughly 100 Hz. A power of typically 3 mW arrives at the hot spot.

In the case of carrier injection through a PC, the technique is slightly different. For each measurement the emitter has to be spot welded to the surface. This is done by applying a voltage of up to 150 V_{dc} via a series resistance of 1 MΩ to the contact. This results in a breakdown of the insulating oxide layer. The discharge of the lead capacitance through the emitter establishes a contact resistance in the order of $R_E \approx 1\Omega$. After spot welding E is fed with an alternating current of constant amplitude (independent of R_E) of typically $I_E \approx 1\text{mA}_{rms}$ at a frequency around 100 Hz. After a measurement is taken at this position, E is broken by simply sliding it to the next position, where the cycle is repeated. In order to perform this procedure without causing too much damage to the sample E is shaped in the form of a hairpin suspended by two wires in a V-shaped arrangement. After mechanical contact of E and the sample, the scanner is gently pushed a little bit further in z-direction in order to apply a small pressure to E. Because of its shape (well known from force microscope sensors[4]), the suspension of E is rather soft with respect to deformations in the z-direction, but quite stiff with respect to forces in the x- and y-directions. Thus E follows rigidly the x- and y-movement imposed by the scanner, but at the same time it rides softly over the surface.

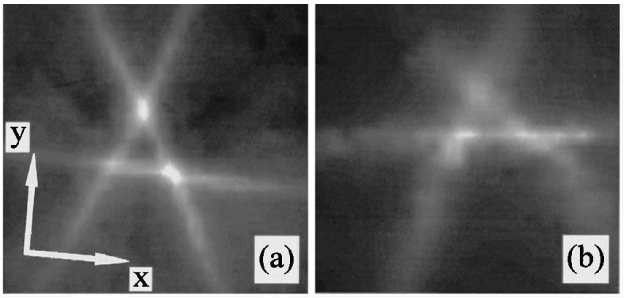

FIG. 5. Experimental result obtained by (a) the illumination of the hot spot on the c-(trigonal) surface of a Bi single crystal slab with $d=0.5$ mm thickness and (b) by the injection of a current through an emitter point contact on a Bi sample of $d=0.25$ mm thickness. V_C is displayed in grey scale as a function of the position of the hot spot or E, respectively: (a) the image frame is $(1\ \text{mm})^2$ resolved by (50×50) (raw) data, $6\ \text{nV}_{\text{rms}} \leqslant V_C \leqslant 20\ \text{nV}_{\text{rms}}$. x and y denote the binary and the bisectrix axis of Bi, respectively, (b) the image frame is $(0.5\ \text{mm})^2$ resolved by (25×25) (raw) data, $I_E=10\ \text{mA}_{\text{rms}}$, $0.5\mu\text{V}_{\text{rms}} \leqslant V_C \leqslant 0.6\mu\text{V}_{\text{rms}}$.

The collector PC is spot welded to the opposite surface of the sample and remains fixed during both types of measurements. The typical signals at C with respect to a reference contact at one of the edges of the sample slab are of the order $V_C \approx 100\ \text{nV}_{\text{rms}}$. They are detected by standard lock in techniques. Scanning of the source (hot spot or E) with the detector (C) fixed is equivalent to a fixed source and a scanned detector, if homogeneity of the sample and its surfaces can be assumed. The data presented here can therefore simply be interpreted as the far field radiation pattern of a pointlike source located behind the viewing window.

The direction of motion of an electron is given by its group velocity $\mathbf{v}_{\text{gr}}(\mathbf{k})=\hbar^{-1}\nabla_k E(\mathbf{k})$; here $\mathbf{k}$ is the wave vector of the electron, $\hbar=h/(2\pi)$, h is Planck's constant and $E(\mathbf{k})$ is the electronic band structure. The Fermi surface (FS) is a surface of constant energy, namely the Fermi energy E_F, so $\mathbf{v}_{\text{gr}}$ is perpendicular to the FS for all electrons at the FS. If regions in k-space with small (or even vanishing) FS-curvature exist, the electron current density will exhibit maxima (or even singularities) along the group velocity directions associated to these regions since here many group velocity vectors point in (nearly) the same direction. This phenomenon is called electron focusing (EF) in analogy to the well known effect of phonon focusing (PF). The FS of Bi is composed of three electron ellipsoids and one hole ellipsoid. The electron ellipsoids transform into one another by rotation around the k_z-axis by 120°, their longest axis is inclined by 6° against the $(k_x k_y)$-plane.[20] They are extremely stretched (15:1) and can be approximated as cylinders; EF is therefore expected to occur in planes perpendicular to the longest axes of these ellipsoids.

Two examples for results are shown in Fig. 5(a) and 5(b) for thermal excitation and carrier injection. The samples were in the form of thin slabs with their large surfaces perpendicular to the c- (k_z-) direction of the crystal. In both cases the three bright lines result from the above-mentioned focusing of the electrons. The EF lines show up where the focusing planes cut the surface plane of the sample. In the case of thermal excitation a second structure of opposite polarity is visible. It originates from the focusing of slow transverse phonons. They are detected by the PC because they apparently couple to the holes via phonon drag.[21] So the EF pattern in Fig. 5(a) represents a thermoelectric signal in the ballistic limit showing the different contributions to the thermopower of Bi (ballistic counterpart of the diffusion term and phonon drag term). Since the power dissipated in E by carrier injection is small compared to that one dissipated in the hot spot (typically 1 μW), the phonons do not show up in Fig. 5(b). This second version of our EF experiment offers in principle the possibility of spatially (angular) resolved spectroscopic measurements, since V_E defines the excess energy, with which the electrons are injected into the sample. In this way one might perform experiments to study the anisotropy of band structure-related features (superconductor energy gaps, effective masses, carrier lifetimes) of interesting materials.

Further details about this experiment can be found in Ref. 19.

V. CONCLUSIONS

We have presented a versatile mechanical micropositioning unit offering positioning in three dimensions along three orthogonal directions up to the mm range with a precision and reproducibility in the μm range. Its design is compact and simple and its operation is intuitive and straightforward due to the orthogonal construction principle. It can be scaled up (or down) to have access to larger (or smaller) scan ranges. A spring reduction system[15] can easily be incorporated for high precision positioning. Since it is entirely constructed from nonmagnetic materials, it can be used in magnetic fields and in cryogenic environments. It was originally designed for point contact experiments but it might be useful in any application, where movements of samples or probes within the specifications given in the article are needed, for example as a coarse positioning unit or scanning unit in any kind of scanned probe microscope. The performance of the system is demonstrated by the presentation of an experiment investigating electron focusing in a Bi single crystal slab, where the unit was used to position and raster-scan different probes with respect to each other and the sample at a temperature of $T=1.5$ K.

ACKNOWLEDGMENTS

We are most grateful to J. Dettinger, H. Dresler, R. Pankow and J. Spitznagel for their expert technical assistance during the construction and the stepwise improvements of the scanner, which was of primary importance for the accomplishment of this work. We wish to thank E. Schönherr, H. Wendel and H. Bender from M.P.I.-Stuttgart for the supply of the Bi samples.

[1] Y. Kuk and P. J. Silverman, Rev. Sci. Instrum. **60**, 165 (1989).
[2] H. Fuchs, Phys. Blätter **50**, 837 (1994).
[3] G. Binnig, H. Rohrer, Ch. Gerber, and E. Weibel, Appl. Phys. Lett. **40**, 178 (1982).
[4] D. Sarid and V. Elings, J. Vac. Sci. Technol. B **9**, 431 (1991).
[5] U. Dürig, D. Pohl, and F. Rohner, IBM J. Res. Dev. **30**, 478 (1996).

[6] P. Günther, U. Ch. Fisher, and K. Dransfeld, Appl. Phys. B **48**, 89 (1989).
[7] L. N. Vu, M. S. Wistrom, and D. J. van Harlingen, Appl. Phys. Lett. **63**, 1693 (1993).
[8] A. M. Chang, H. D. Hallen, H. F. Hess, H. L. Kao, J. Kwo, A. Sudbø, and T. Y. Chang, Europhys. Lett. **20**, 645 (1992).
[9] A. M. Chang, H. D. Hallen, L. Harriott, H. F. Hess, H. L. Kao, J. Kwo, R. E. Miller, R. Wolfe, and J. van der Ziel, Appl. Phys. Lett. **61**, 1974 (1992).
[10] R. Mäckel, H. Baumärtner, and J. Ren, Rev. Sci. Instrum. **64**, 694 (1993).
[11] R. C. Black, F. C. Wellstood, E. Dantsker, A. H. Miklich, J. J. Kingston, D. T. Nemeth, and J. Clarke, Appl. Phys. Lett. **64**, 100 (1994).
[12] B. Cretin and F. Sthal, Appl. Phys. Lett. **62**, 829 (1993).
[13] J. Siegel, J. Witt, N. Venturi, and S. Field, Rev. Sci. Instrum. **66**, 2520 (1995).
[14] D. A. Brawner and N. P. Ong, J. Appl. Phys. **73**, 3890 (1991).
[15] R. N. Goren and M. Tinkham, J. Low Temp. Phys. **5**, 465 (1971).
[16] I. R. Smith, R. A. Harvey, and D. J. Fathers, IEEE Trans. Sonics Ultrason. **SU-32**, 274 (1985).
[17] H. F. C. Hoevers, J. G. H. Hermsen, and H. van Kempen, Rev. Sci. Instrum. **60**, 1316 (1989).
[18] Torr Seal, available from Varian Associates.
[19] J. Heil, M. Primke, K. U. Würz, and P. Wyder, Phys. Rev. Lett. **74**, 146 (1995).
[20] V. S. Edelman, Adv. Phys. **25**, 555 (1976).
[21] R. D. Barnard, *Thermoelectricity in Metals and Alloys* (Taylor & Francis, London, 1972).